

MICROWAVE INSTABILITY STUDIES IN NSLS-II*

A. Blednykh[#], B. Bacha, G. Bassi, W. Cheng, O. Chubar, K. Chen-Wiegart, V. Smaluk
BNL, NSLS-II, Upton, NY, 11973-5000, USA

Abstract

The microwave instability in the NSLS-II has been studied for the current configuration of insertion devices, 9 In-Vacuum Undulators (IVU's), 3 Elliptically-Polarized Undulators (EPU's), 3 Damping Wigglers (DWs). The energy spread as a function of single bunch current has been measured based on the frequency spectrum of IVU for X-Ray Spectroscopy (SRX) beamline, for two lattices, the bare lattice with nominal energy spread $\sigma_\delta = 0.0005$, and a lattice with one DW magnet gap closed ($\sigma_\delta = 0.0007$). In addition we did measure the energy spread from a Synchrotron Light Monitor (SLM) camera installed in a nonzero dispersive region, for the two aforementioned lattices, and for a third lattice with 3 DWs gaps closed ($\sigma_\delta = 0.00087$). The measurements have been complemented by beam spectra taken from a Spectrum Analyzer, and have been compared with numerical simulations with the particle tracking code SPACE.

MEASUREMENTS

The NSLS-II storage ring has been designed to accumulate a high-current (500 mA) electron beam with sub-nanometer (0.5 nm with all damping wigglers) horizontal emittance and diffraction-limited vertical emittance smaller than 8 pm [1]. Three pairs of damping wigglers have been installed in NSLS-II in Cells 8, 18 and 28 to decrease the horizontal emittance below 1 nm. The wigglers introduce additional strong radiation damping which increases the beam energy spread and the bunch length. The magnet gaps of the wigglers and insertion devices are controlled remotely; this allows us to vary the lattice configuration with any ID's combination.

Three different diagnostic methods have been used in parallel to determine the longitudinal microwave instability threshold in NSLS-II. Horizontal beam-profile changes vs single bunch current have been monitored by a SLM camera installed in a low dispersion area (Fig. 1). IVU of a SRX beamline has been used as a diagnostic tool to determine the energy spread based on the spectral peak of the 5th harmonic radiation as a function of current (Figs. 2, 3). A reliable estimation of the electron beam energy spread from SRX IVU photon energy spectrum became possible after careful re-alignment of the IVU magnet girders with respect to the electron beam. The third method is based on beam spectrum measurements from the stripline of a bunch-by-bunch transverse feedback system. The monitor of a spare stripline was connected to the RF- input of an ESA 4405B spectrum analyzer. The center frequency was set to the 21th RF

harmonic (10493.3136MHz) with a span of 40KHz. It was verified to be the most sensitive span for the synchrotron sidebands. This method is used at other facilities [2], besides being used at NSLS-II [3]. The longitudinal instability thresholds have been studied for three different lattices, a bare lattice (all ID's gap open), a lattice with 1DW magnet gap closed and a lattice with 3DWs magnet gap closed. By closing the DWs magnet gap we measured the microwave instability threshold current I_{th} dependence on the energy spread σ_δ at fixed RF voltage (Figs. 1-5). Based on the measurements, we observed the expected dependence $I_{th} \propto \sigma_\delta^3$. The measured I_{th} from both SLM and SRX beamline has been found to be $I_{th} \sim 0.2 - 0.3$ mA (bare lattice) [3], $I_{th} \sim 0.8 - 0.9$ mA (1 DW gap closed), and $I_{th} \sim 1.6$ mA (3 DWs gaps closed) respectively, as shown in Figs. 1 and 2. The thresholds have been confirmed from the measured beam spectra shown in Figs. 4 and 5, where the second harmonic of the synchrotron frequency f_s suddenly appears at the microwave instability threshold. Measurements from SLM for the lattice with 3 DWs gap closed are shown in Fig. 6 at $V_{RF} = 2$ MV, $V_{RF} = 2.6$ MV and $V_{RF} = 3.4$ MV.

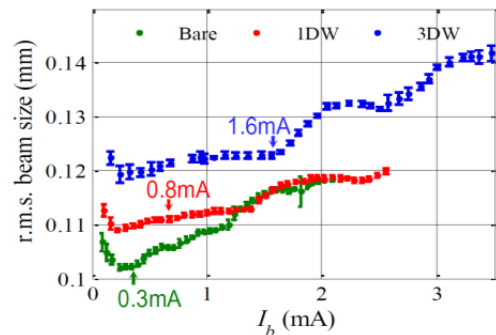


Figure 1: Horizontal beam size from SLM vs single bunch current for three different lattices at $V_{RF} = 2.6$ MV.

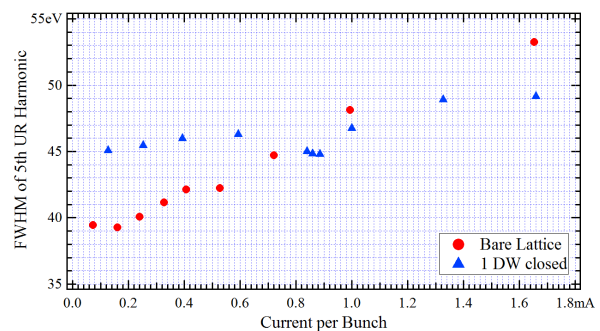


Figure 2: FWHM size of spectral peak of 5th harmonic radiation from 21-mm period IVU measured at SRX beamline at ~ 8 keV photon energy as a function of current per bunch, for bare lattice and with one DW closed.

* Work supported by Department of Energy contract DE-AC02-98CH10886

[#]blednykh@bnl.gov

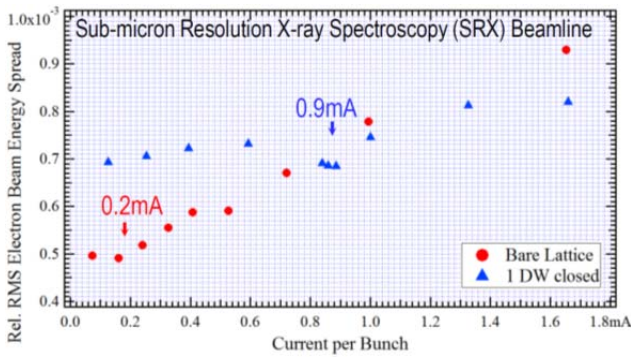


Figure 3: RMS electron energy spread as a function of current per bunch for bare lattice and with one DW closed, estimated from the 5th harmonic size measurements illustrated in Fig. 2.

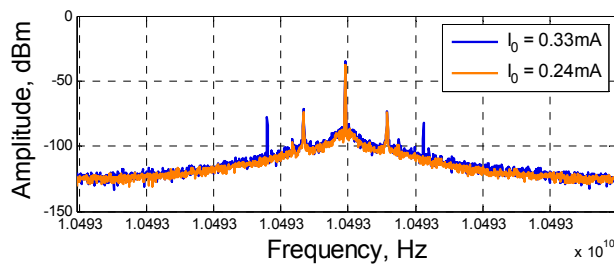


Figure 4: Measurement of beam spectrum for bare Lattice. $V_{RF} = 2.6\text{MV}$.

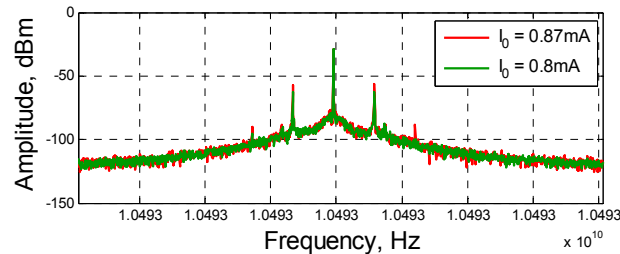


Figure 5: Measurement of beam spectrum for lattice with 1 DW magnet gap closed. $V_{RF} = 2.6\text{MV}$.

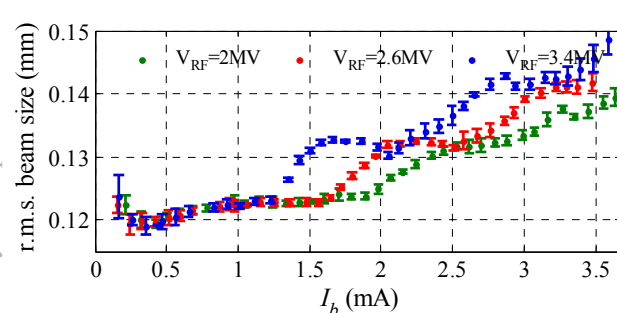


Figure 6: Horizontal beam size change vs single-bunch current monitored by SLM camera for a lattice with 3DW's magnet gap closed at different RF Voltage: $V_{RF} = 2\text{MV}$, $V_{RF} = 2.6\text{MV}$ and $V_{RF} = 3.4\text{MV}$.

NUMERICAL SIMULATIONS

Numerical simulations with SPACE have been done for the lattice with 3 DWs gaps closed. We use a sum of two broadband resonators (BBRs) with parameters listed in Table 1 as the impedance model. The numerical simulations are done using 30M simulation particles and 800 grid points in order to accurately determine the microwave instability threshold, and to characterize the dynamics above it. Figure 7 shows the maximum amplitude energy spread as a function of single bunch current at several values of the RF voltage in the range 1.1MV-3.4MV. The maximum amplitude of the energy spread oscillations is determined by inspecting the last 5000 turns of the bunch time evolution. This is shown in Figs. 8 and 9 for $V_{RF} = 2.6\text{MV}$ and $V_{RF} = 3.4\text{MV}$ respectively.

Table 1: NSLS-II Broad-Band Impedance Model

f_r , GHz	$R_{sh, }$, k Ω	Q
20	8	4
58	4.3	3.5

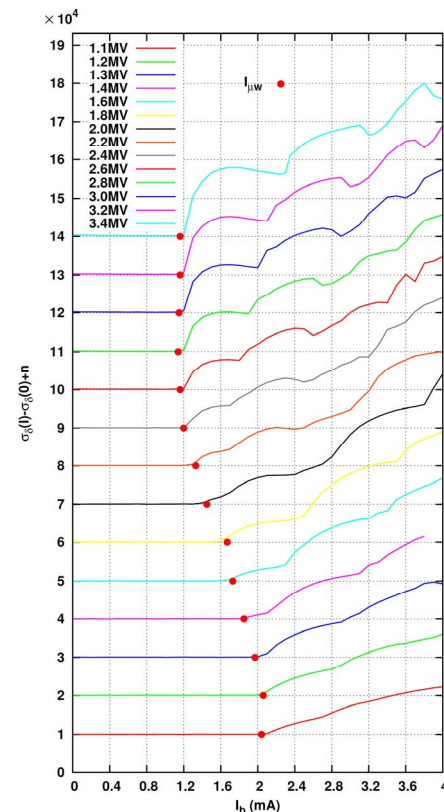


Figure 7: Numerical simulations of the energy spread vs. single bunch current at different RF voltages for the lattice with 3 DWs magnet gaps closed. In the vertical axis to the energy spread as a function of current is subtracted the value at zero current, and added a constant offset n ($n=1, \dots, 14$) for a better display of the results. The red points label the microwave instability threshold, here shown as $I_{\mu w}$.

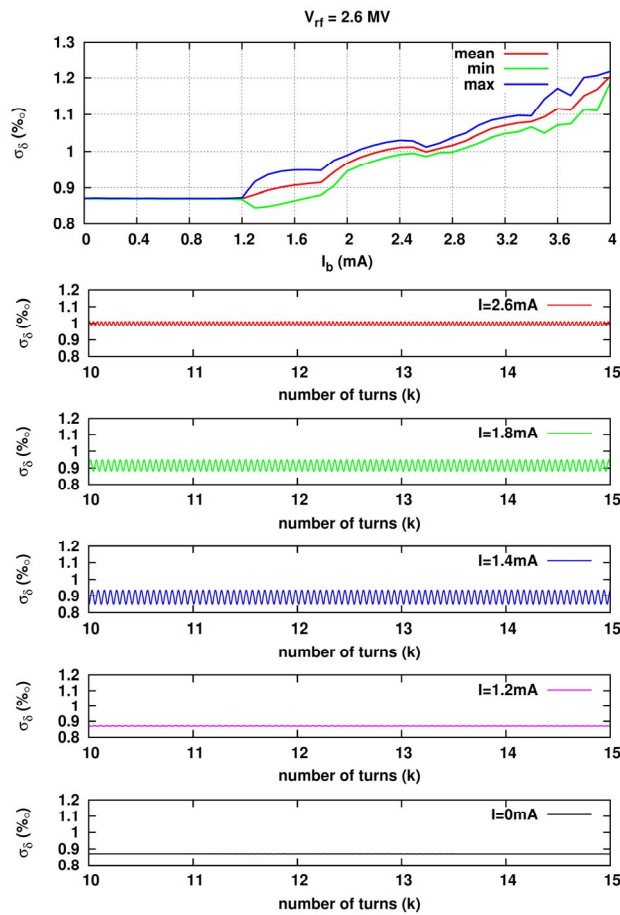


Figure 8: The top frame shows the mean (red line), maximum (blue line), and minimum (green line) of the amplitude of the energy spread as a function of single bunch current over the last 5000 turns of the bunch evolution. The other frames show the energy spread evolution over the last 5000 turns at different sing bunch currents. Notice that the range of oscillation of the energy spread is not increasing monotonically with bunch current. The results shown are for $V_{RF} = 2.6\text{MV}$.

In Fig. 10 the numerical results are compared with measurements, where lines correspond to numerical results, and points to measurements. The red points label the microwave instability threshold at the different RF voltages. Above the microwave instability threshold, we notice several transition thresholds at which the functional dependence of the energy vs bunch current changes in shape. A characterization of the patterns shown in Fig. 8,9,10 is under investigation.

SUMMARY

Multiple longitudinal instability thresholds have been observed at NSLS-II. Preliminary simulations using a BBR model show approximate agreement with the measured data. The measured microwave instability threshold is proportional to the cube of the energy spread, $I_{th} \propto \sigma_{\delta}^3$, and follows approximately the dependence

$I_{th} \propto 1/\sqrt{V_{RF}}$, according to the Keil-Schnell-Boussard criterion.

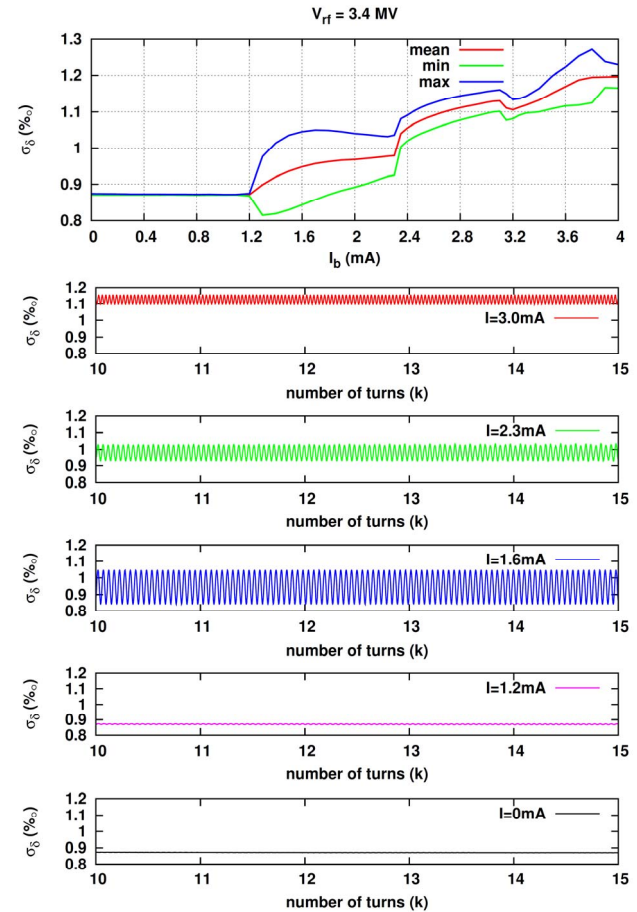


Figure 9: Same as Fig. 8 for $V_{RF} = 3.4\text{MV}$.

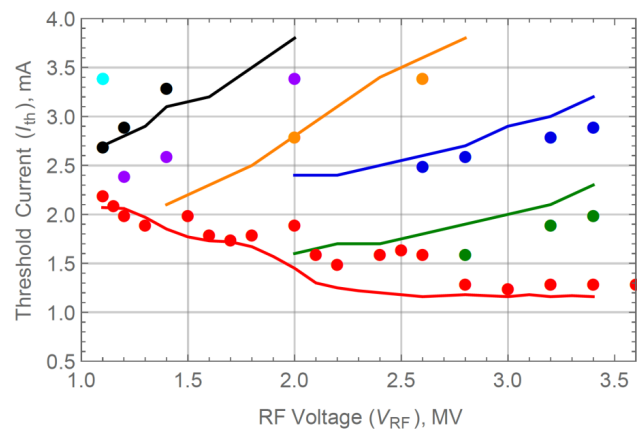


Figure 10: The single-bunch longitudinal microwave instability threshold vs RF voltage (3 DWs lattice) is shown in red. Traces in color different from red indicate thresholds higher than the microwave instability threshold at which the functional dependence of the energy on the bunch current changes in shape. Dots correspond to measurements, lines to numerical simulations.

REFERENCES

- [1] NLSL-II Conceptual Design Report, December 2006.
- [2] Y.-C. Chae, L. Emery, A.H. Lumpkin, J. Song, B.X. Yang, in *Proc. of PAC2001*, Chicago, IL, USA, May 2001, paper TPPH068, p. 1817.
- [3] W. Cheng, B. Bacha, G. Bassi, A. Blednykh, B. Podobedov, O. Singh, V. Smalyuk, in *Proc. of IPAC2016*, Busan, Korea, May 2016, paper TUPOR033, p. 1738.